Hindawi
Journal of Chemistry
Volume 2019, Article ID 3869732, 7 pages
https://doi.org/10.1155/2019/3869732

Research Article

Formation of Incrustations during the Cocombustion of Biomass in Fluidised Bed Boilers

Petr Buryan

Department of Gaseous and Solid Fuels and Air Protection, University of Chemistry and Technology Prague, Technická 5, 166 28 Praha 6, Czech Republic

Correspondence should be addressed to Petr Buryan; buryanp@vscht.cz

Received 6 May 2019; Revised 18 July 2019; Accepted 29 August 2019; Published 16 October 2019

Academic Editor: Kaustubha Mohanty

In this article, we focus on causes of formation of incrustations in fluidised bed boilers that result from combustion of biomass-containing energy-producing raw materials and can significantly limit the efficiency of the respective power equipment operation. We applied laboratory procedures followed for assessment of characteristic eutectics of mixtures of coal ashes, desulphurisation components (dolomite and limestone), and woodchip ashes. Our analysis proved that combustion of these (or similar) raw materials, accompanied by repeated heating and cooling of combustion and flue gas desulphurisation products, leads to the formation of unfavourable incrustations. These incrustations can grow up to several tens of centimetres in size, thereby significantly restricting the power equipment functionality. They arise due to incrust reheating that results in the formation of eutectics, which have lower melting temperatures than that during their first pass through the combustion process. The same holds for desulphuriation components themselves. Formation of these new eutectics can be attributed both to recycling of substances produced during the first pass through the furnace as well as to mixtures formed both from recycled materials and from components initially combusted in the boiler furnace.

1. Introduction

Increased support of the use of biomass and wastes of diverse origin for energy purposes has caused many unexpected problems in power engineering. Many of the issues began to appear mainly in connection with sintering of the ashes of these materials in furnaces and in related technologies. One of the strongly affected areas is cocombustion of biofuels and coal in circulating fluidised bed boilers (Figure 1). Size of incrustations forming here can range up to several tens of centimetres in size (Figure 2). Two main characteristics of these incrustations are as follows:

(i) Presence of glass phase (see Table 1 for the composition of the connecting glass phase)

(ii) Large quantity of bubbles associated with gas release in a pyroplastic state of ashes

Gas release is connected with carbonate thermolysis [1] and with the reaction between recycled sulphates and unburnt carbon, i.e., with recycling of the components captured from the flue gases in the cyclone back to the boiler furnace:

$$2CaSO_4 + C \longrightarrow 2CaO + 2SO_2 + CO_2 \quad (1)$$

This article focuses on one of the issues we see in desulphurisation of the flue gas during combustion of biofuels in fluidised bed furnaces (with combustion temperatures around $850 \pm 20^{\circ}C$, decreasing to ca $650 \pm 20^{\circ}C$ in recycling cyclones). Cocombustion of biofuels (including alternative ones also containing communal waste) in these appliances brings along several issues connected with coating of the surfaces of limestones and dolomites used for flue gas desulphurisation [2–8]. The most significant effect of the coating is the increase of desulphurisation costs and the quantity of energy by-products containing a nonnegligible amount of unreacted (free) CaO [9–14].

Fluidised bed combustion process usually involves repeated heating of the ash mixtures to high temperatures

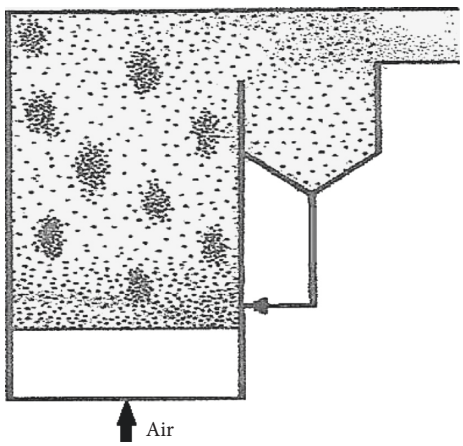

Figure 1: A fluidised bed boiler with a circulating layer.

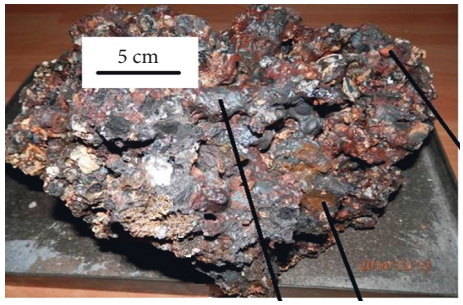

Figure 2: Incrustation from the cocombustion of brown coal and woodchips in a fluidised bed boiler.

Table 1: Composition of the glass parts of the incrustation, wt. %.

Sampling place	A	B	C
Oxide			
Na_2O	0.46	0.13	0.26
MgO	1.73	21.10	0.94
Al_2O_3	21.96	11.35	28.00
SiO_2	45.69	37.35	54.60
K_2O	1.10	0.61	1.55
CaO	12.07	1.20	1.76
Fe_2O_3	13.20	25.63	10.05

followed by their subsequent cooling. One of the main causes of the coating issue is low melting temperatures of mixed ashes (MTMA). This temperature is defined as the temperature at which physicochemical changes occur in the ash structure [7, 15, 16] and can be determined using differential thermal analysis to measure the endomaxima of heated ashes (the approach we also took in this paper). One of the key factors that influence MTMA is whether the material has been previously heated or not. Repeated heating yields mixtures of components that can be formed only at higher temperatures enabling their subsequent mutual reactions as well as their reactions with pyroplastic components produced during the first heating. In effect, the resulting material has a different structure and also different MTMA compared to the nonheated one.

2. Materials and Methods

In our experiments, we tried to mimic this reheating process by repeatedly heating the prepared ash samples after cooling them to room temperature. It must be noted here that the actual process of ash acquisition can significantly impact the results of MTMA assessment as thermolysis may involve various chemical transformations. Therefore, a special attention in our research was given to the preparation of the analysed energy by-products [9, 15, 16].

The set of samples analysed in this study consisted of limestone (L) from the lime works Vápenka Čertovy schody (Barrandian Palaeozoic, Czech Republic (CZ)), dolomite (D) from the quarry of Kamenolom Nové Mesto nad Váhom, Slovak Republic (SR), brown coal (C) from the Bílina mine (North Bohemian Mines, CZ), and raw woodchips from CEZ power stations with chip size 0.3–3 cm, 95% wt.

We selected the raw material grain size of 0.3–0.6 mm based on the working conditions of the laboratory apparatus used in the experiment. The basic parameters of the brown coal, woodchips, and desulphurisation components are listed in Tables 2 and 3.

Purity of the dolomite ($CaMg(CO_3)_2$) shown by carbon content was 12.91 wt. %, and the limestone ($CaCO_3$) purity was 11.94 wt. %. Elemental analyses were performed on a Thermo Scientific Flash 1112 elemental analyser employing Dumas gas chromatography. Ash composition was determined using the RTG spectrometer ARL 9400 XP+ with a detection limit of 3%.

From the whole range of results achieved in our work, this paper presents data concerning the basic parameters of woodchip ashes obtained by targeted combustion at 500°C and 600°C. Selection of these temperatures was intentionally set at levels 50°C above and 50°C below the temperature of 550°C that is recommended by the standards [15, 17–19].

Table 4 shows the model behaviour of the sample raw materials, which were repeatedly heated to the selected temperatures (selection of temperatures was driven by temperatures typically observed in the circulating fluidised bed boilers).

The incrustation formation is caused by creation of diverse eutectics from the ashes of both incinerated energy-producing raw materials and desulphurisation components fed into fluidised bed boiler furnaces. For our experiment, we used ashes that were acquired separately at the temperatures of 500°C and 600°C (see sample definitions in Table 4). Using these samples, eutectic formation was observed as the ashes were repeatedly heated up to 1050°C at a gradient of 10°C/min at the synthetic airflow of 20 ml/min heating in a Pt cup. Cooling after the first cycle was realized by identical flow of helium. The temperatures at which eutectics formed during the first and second heating of the ashes are depicted in Figures 3–7. The differential thermogravimetric analyses (DTA), which characterizes continuously changing temperature of the heated sample relative to the Pt crucible, were performed on a Stanton-Redcroft TG-750 instrument. The possible reaction of the chilled sample with carbon dioxide in the

Table 2: Coal and woodchip parameters, wt. %.

	Raw woodchips	Raw coal
Parameter		
W^r	46.11	22.52
A^r	2.55	10.69
Element		
C^r	26.31	56.54
H^r	3.09	4.58
N^r	0.24	0.95
$S^{r,*}$	0.05	0.36

S*: combustible sulphur.

Table 3: The composition of power and desulphurisation component ashes, wt. %.

Raw material Temperature*	Woodchip ashes 500°C	Woodchip ashes 600°C	Coal ashes 850°C	Limestone 850°C	Dolomite 850°C
Oxide					
Na_2O	0.63	0.58	0.91	0.15	0.19
MgO	3.98	4.16	1.77	0.78	38.40
Al_2O_3	7.26	7.60	33.74	0.87	2.60
SiO_2	32.32	39.47	43.30	2.17	2.33
P_2O_5	3.05	3.49	0.23	0.15	—
SO_3	8.13	2.27	5.24	0.07	0.43
Cl	0.12	0.53	—	0.03	0.03
K_2O	6.98	9.33	1.18	0.11	0.22
CaO	30.75	25.69	4.47	95.20	55.69
TiO_2	0.64	0.67	2.01	0.06	0.02
V_2O_5	0.01	0.01	0.08	—	—
Cr_2O_3	0.01	0.01	0.03	—	—
MnO	1.91	2.47	0.06	0.03	—
Fe_2O_3	3.70	3.66	6.68	0.32	0.06
CuO	0.02	0.02	0.02	—	—
ZnO	0.15	0.14	0.02	—	—
Rb_2O	0.02	0.02	—	—	—
SrO	0.09	0.07	0.06	0.06	0.02
ZrO_2	0.02	0.03	0.06	—	—
BaO	0.22	0.24	0.06	—	—
NiO	0.02	0.01	—	—	—

*: combustion temperature.

Table 4: The designation of model substances.

	Character	Ratio—%	Label
Combustion temperature 500°C			
Woodchips		100	W500
Coal		100	C500
Limestone		100	
Dolomite			
Mixture 1	Limestone + woodchip ashes	50 : 50	LW500
Mixture 2	Coal ashes + woodchip ashes	50 : 50	CW500
Combustion temperature 600°C			
Coal		100	C500
Woodchips		100	W600
Limestone		100	L600
Dolomite		100	D600
Mixture 3	Limestone + woodchip ashes	50 : 50	LW600
Mixture 4	Coal ashes + woodchip ashes	50 : 50	VW600

second heating associated with its release was eliminated by serial connection of thermodynamic weights with a mass spectrometer OmniStar™, Pfeiffer Vacuum.

We organised our experiment in four phases, measuring the reheating behaviour of the individual substances (isolated) in the first two and then assessing the behaviour of

mixtures. Within each phase, we heated and reheated the samples and measured their respective endomaxima. Individual objectives of each phase were as follows:

(1) Understanding the behaviour of desulphurisation materials during reheating: we (re-) heated only limestone and dolomite (samples L and D, resp.) to measure raw material behaviour without impact of ashes (Figures 3 and 4) (cooling after the first cycle was realized by the flow of helium; the reason why we decided to do so was our intention to avoid reversal reaction of CO_2 with air)

(2) Understanding the behaviour of ashes during reheating: we (re-) heated coal ashes (C500) and a mixture of coal ashes with woodchip ashes (CW500 and CW600) to measure the behaviour of ashes without limestone (Figure 5)

(3) Understanding the impact of mixing ashes with limestone: we (re-) heated limestone mix and woodchip ashes (W500 and W600) and the woodchip ash (LW500) to understand the impact of ashes on limestone behaviour during reheating (Figures 6 and 7)

(4) Assessing the influence of Fe_2O_3: we (re-) heated two mixtures, one of limestone + Fe_2O_3 (1 : 1) and the second of limestone + woodchips + Fe_2O_3 (1 : 1 : 1)—to verify the influence of high Fe_2O_3 content in woodchip ashes on the formation of aluminosilicates (Table 1 for Fe_2O_3 sample definition)

2.1. Behaviour of Desulphurisation Materials during Reheating. Figure 3 clearly illustrates the difference between endomaxima of the first and repeated limestone heatings. An endomaximum of only 680°C was reached during repeated heating of sole calcined limestone. This temperature is 140°C lower than the endomaximum level of the first heating recorded at ca 820°C.

2.2. Behaviour of Ashes during Reheating. Figure 4 shows the heating behaviour of the studied dolomite that yielded two endomaxima. The first heating yielded endomaxima at ca 800°C and 845°C. During repeated heating, the two endomaxima shifted to lower temperatures of ca 405°C and 705°C. Figure 5 clearly shows that addition of woodchips to coal ashes leads to undesirable reactions with the endomaxima around 730–750°C. Note that when the brown coal ashes (obtained at 600°C) were heated alone, no eutectic was recorded up until 1050°C.

2.3. Impact of Mixing Ashes with Limestone. When comparing the eutectics of ashes acquired at 500°C and 600°C (Figures 6 and 7), it is evident that the eutectic of the 600°C woodchip ash achieves its maximum at temperature ca 15°C below the eutectic of the 500°C woodchip ash. Addition of the 500°C woodchip ash clearly reduces the limestone eutectic by ca 30°C. In contrast to this, no formation of eutectic

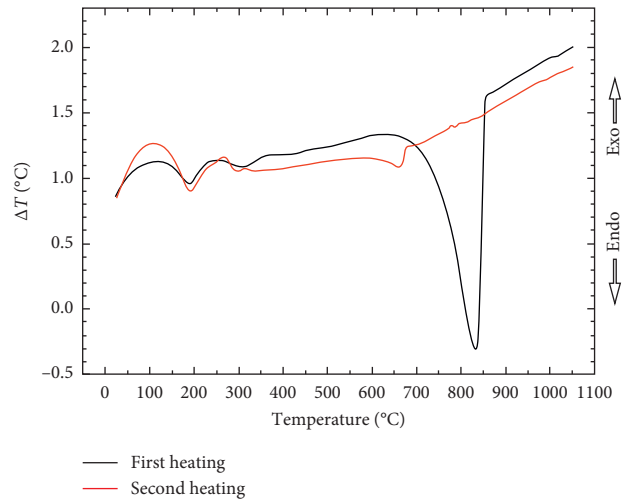

Figure 3: Comparison of DTA heating curves of sample L600.

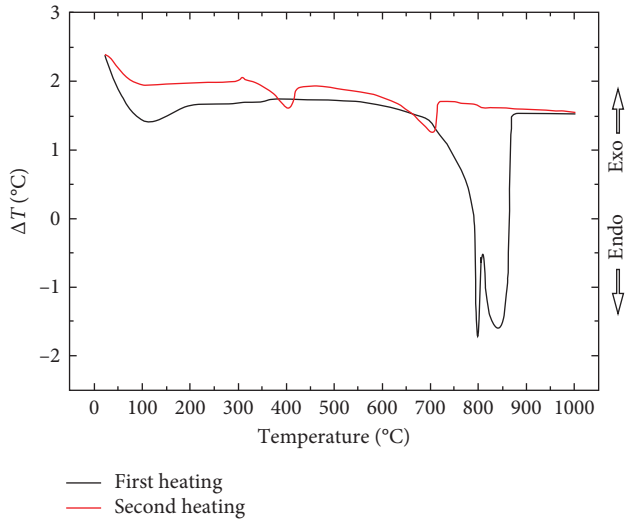

Figure 4: Comparison of DTA heating curves of sample D600.

has been observed during repeated separate heating of both woodchip ash samples.

Interesting results came from repeated heating of calcined limestone and its mixture with woodchip ashes that have already been once heated to 1050°C. Reheating of limestone alone forms a new eutectic at a temperature lower by ca 180°C. This means that the first heating led to formation of such components that create eutectic at a much lower temperature when the limestone is heated again. The same holds for repeated heating of the mixture of woodchip ashes and limestone. Also in this case (when the mixture is heated to 1050°C for the second time), the products of the first thermolysis form a new eutectic at lower temperature levels of ca 645°C.

Based on these observations, it is reasonable to assume that the components produced in combustion associated with recirculation can form mixtures melting at significantly lower temperatures upon their reentry into the furnace after cooling (compared to melting temperatures of the first

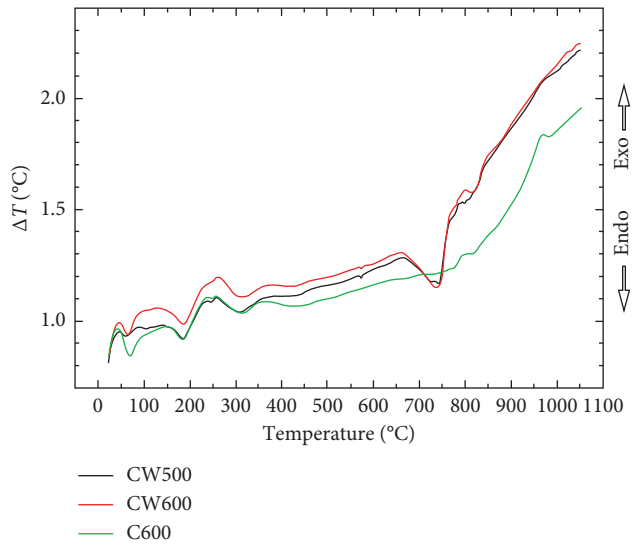

Figure 5: Comparison of DTA curves depicting the influence of woodchip ashes on the formation of coal ash eutectics, the first heating.

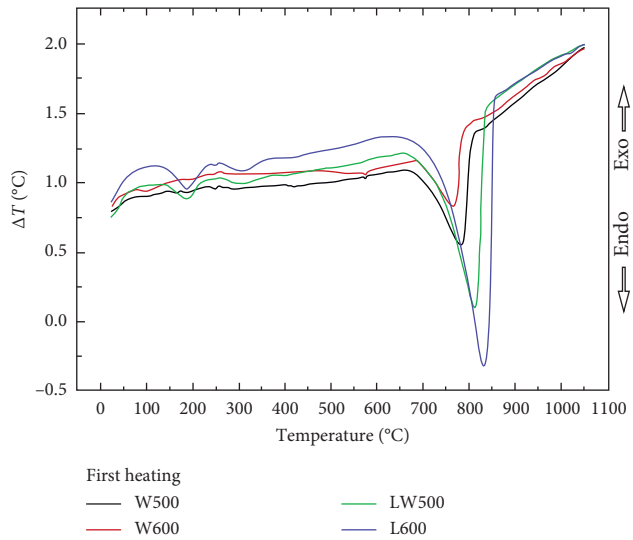

Figure 6: Comparison of DTA curves of the first heating.

combustion cycle). Recycling thus negatively affects the desulphurisation efficiency of fluidised bed boilers during the cocombustion of brown coal and biomass.

Changes in the crystalline phase of the monitored samples after the second heating were monitored by X-ray diffraction analysis. This was performed on a PANalytical X'Pert PRO powder diffractometer at room temperature. The data were evaluated using the High Score Plus software. The results of analyses are summarized in Tables 5 and 6, in which the crystalline components are recorded using the so-called score or percentage probability.

2.4. Assessing Influence of Fe_2O_3. The last step of the experiment was verification of the influence of high Fe_2O_3 content in woodchip ashes on the formation of aluminosilicates. For this purpose, our experimental investigation was complemented by heating of two mixtures: limestone + Fe_2O_3 (1 : 1) and limestone + woodchips ashes + Fe_2O_3 (1 : 1 : 1) (see Table 1 for samples definition). Both were heated to 850°C. Analysis of reaction products after cooling showed presence of incrustations, and XRD analyses (X'Pert PANalytical X'Pert PRO) discovered presence of compounds of the $CaO.Al_2O_3.Fe_2O_3$ type. Alkalis of the $K_2O.CaO.SiO_2$ type were identified as well [20].

These XRD results clearly prove considerable influence that alkali oxides with high concentration in biomass ashes have on incrustation formation. In the assessment of the role of Fe_2O_3, it is also necessary to bear in mind the influence of the sulphur components contained in brown coal, for example, pyrite and clay contained in both coal and desulphurisation substances [21].

In our work, we focused on formation of incrustations that result from combustion of biomass-containing energy-producing raw materials. Laboratory procedures followed in the assessment of characteristic eutectics of mixtures of coal ashes, desulphurisation components, and biomass ashes

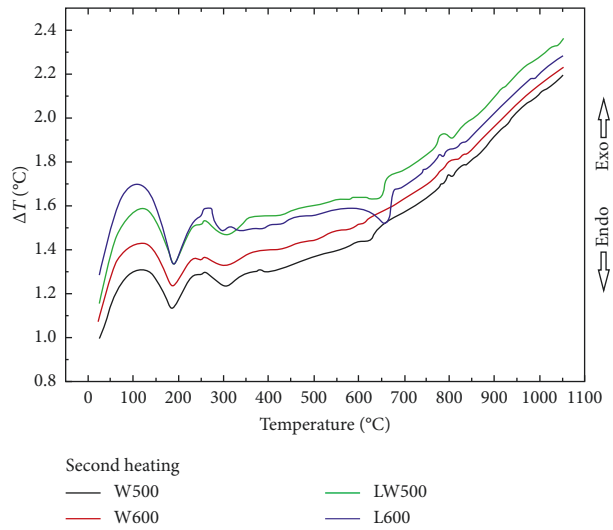

Figure 7: Comparison of DTA curves of the second heating.

Table 5: Analysis of the crystalline phase after the 1st and 2nd heating.

Vzorek Složení	Anhydrite $CaSO_4$	Albite $Na_{0,84}Ca_{0,16}Al_{1,16}Si_{2,84}O_8$	Larnite $Ca_2\ SiO_4$	Gehlenite $Ca_2Al(AlSiO_7)$	Garnet $Ca_3Al_2Si_3O_{12}$
1. Heating	**14**	—	**15**	**8**	—
2. Heating	**17**	**21**	**16**	**12**	**2**

Table 6: Analysis of the crystalline phase after the 1st and 2nd heating.

Vzorek Složení	Hematite Fe_2O_3	Nacrite $Al_2Si_2O_5(OH)_4$	Lime CaO	Quartz SiO_2	Nepheline $Na_6\ K_{1.2}\ Al_{7.1}\ Si_{8.9}\ O_{32}$
1. Heating	**2**	**13**	**15**	**15**	**19**
2. Heating	**5**	—	**7**	**5**	**10**

clearly proved that the fluidised bed combustion of these raw materials produces substances capable of forming unfavourable incrustations of sizes that can significantly limit the efficiency of the concerned power equipment operation.

3. Conclusions

By using eutectic techniques to blend coal ash, desulphurisation components, and biomass ash, it has been shown that, in the fluidized bed combustion process, recycled combustion products produce substances that are capable of producing incrustations of sizes that significantly limit the operation of the power plant.

In recirculation modeling, it was ensured that during cooling, there was no reaction of the oxides formed during the first heating with carbon dioxide to form carbonates.

Data Availability

The experimental data gathered during the laboratory experiments used to support the findings of this study are included within the article.

Conflicts of Interest

The author declares that there are no conflicts of interest.

References

[1] J. G. Yates, *Fundamentals of Fluidised-Bed Chemical Process*, Butterwoth, Oxford, UK, 1983.

[2] P. Buryan, "The influence of alternative solid fuels on desulfurization of fluidized bed boilers," *Chemické Listy*, vol. 109, no. 7, pp. 635–640, 2015.

[3] P. Buryan, J. Vejvoda, J. Krátký, and L. Veverka, "The causation of highconsumption of limestone in coal fluidized bed boiler desulfurization," *Ceramics—Silikáty*, vol. 54, no. 1, pp. 85–88, 2010.

[4] P. Buryan, "The negative effect of biomass Co-combustion on desulfurization ofCombustion products from fluid steam generators," *Chemické Listy*, vol. 108, no. 12, pp. 1162–1167, 2014.

[5] P. Buryan, "Release of gases during the measurement of characteristic temperatures of biomass ash fusibility," *Chemické Listy*, vol. 110, no. 6, pp. 456–459, 2016.

[6] P. Buryan, "The effect of biomass on the compliance with emissions limits in fluidised-bed boiler desulfurisation," *Energy & Fuel*, vol. 31, no. 1, pp. 119–123, 2017.

[7] F. J. Gutiérrez, P. Ollero, A. Cabanillas, and J. Otero, "A technical pilot plant assessment of flue gas desulfurisation in a circulating fluidised bed," *Advances in Environmental Research*, vol. 7, no. 1, pp. 73–85, 2002.

[8] Y. Suyadal, M. Erol, and H. Oguz, "Deactivation model for dry desulphurization of simulated flue gas with calcined limestone in a fluidized-bed reactor," *Fuel*, vol. 84, no. 12, pp. 1705–17012, 2005.

[9] P. Buryan, J. Vejvoda, F. Skacel, and V. Tekáč, "Chlorine balance at brown coal combustion and flue gas desulfurisation," *Polish Journal of Environmental Studies*, vol. 17, no. 5, pp. 687–692, 2008.

[10] F. M. Okasha, S. H. El-Emam, and H. K. Mostafa, "The fluidized bed combustion of a heavy liquid fuel," *Experimental Thermal and Fluid Science*, vol. 27, no. 4, pp. 473–480, 2003.

[11] L. Duau, H. Sun, C. Zhao, W. Zhou, and X. Chen, "Coal combustion on an oxy-fuel circulation fluidized bed combustor with warm flue gas recycle," *Fuel*, vol. 127, no. 1, pp. 47–51, 2014.

[12] F. Scala and P. Salatino, "Flue gas desulfurization under simulated oxyfiring fluidized bed combustion conditions: the influence of limestone attrition and fragmentation," *Chemical Engineering Science*, vol. 65, no. 1, pp. 556–561, 2010.

[13] T. Hlinčik and P. Buryan, "Evalution of limestones for the purposes of desulphurisation during the fluid combustion of brown coal," *Fuel*, vol. 104, no. 2, pp. 206–215, 2016.

[14] L. F. de Diego, M. Obras-Loscertales, L. García Labiano et al., "Characterization on limestone in a batch fluidized bed reactor for sulfur retention under oxy-fuel operating conditions," *International Journal of Greenhouse Gas Control*, vol. 5, no. 5, pp. 1190–1198, 2011.

[15] J. Horák, M. Branc, F. Straka et al., "Problems of determination of characteristic temperatures of biomass ash fusibility," *Chemické Listy*, vol. 107, no. 6, pp. 502–509, 2014.

[16] M. Hartman, O. Trnka, K. Svoboda, and V. Vesely, "Agglomeration of particles and defluidization phenomena in the fluid bed," *Chemické Listy*, vol. 97, no. 9, pp. 942–948, 2003.

[17] ASTM International, *ASTM D 1857–87: Standard Test Method for Fusibility of Coal and Coke Ash*, ASTM International, West Conshohocken, PA, USA, 1994.

[18] Deutsches Institut für Normung, *DIN 51730: Testing of Solid Fuels, Determination of Fusibility of Fuel Ash*, Deutsches Institut für Normung, Berlin, Germany, 2007.

[19] BSI, *DD CEN/TS 15370–1:2006 Solid Biofuels, Method for the Determination of Ash Melting, Behaviour, Characteristic Temperatures Method*, BSI, London, UK, 2006.

[20] P. Buryan, "Gas generation during Cypris clay expansion," *Journal of Thermal Analysis and Calorimetry*, vol. 134, no. 2, pp. 981–992, 2018.

[21] V. Hanykýř and J. Kutzendörfer, *Ceramics Technology*, Silikátový svaz, Praha, Czech Republic, 2nd edition, 2002.